Molecular Crystals and Liquid Crystals
Publication details, including instructions for authors and subscription information:
http://www.tandfonline.com/loi/gmcl20

Experimental and Ab Initio Computational Studies on 4-(Benzhydryloxy)phthalonitrile

Hanife Saraçoğlu [a], Feyizan Güntepe [b], Çiğdem Yüksektepe [c], Nezihe Çalışkan [b] & Sinan Saydam [d]

[a] Department of Middle Education, Educational Faculty, Ondokuz Mayis University, Kurupelit, Samsun, Turkey

[b] Department of Physics, Faculty of Arts and Sciences, Ondokuz Mayis University, Kurupelit, Samsun, Turkey

[c] Department of Physics, Faculty of Science, Çankırı Karatekin University, Ballıca, Çankırı, Turkey

[d] Department of Chemistry, Faculty of Science, Fırat University, Elazığ, Turkey

Version of record first published: 08 Apr 2011

To cite this article: Hanife Saraçoğlu, Feyizan Güntepe, Çiğdem Yüksektepe, Nezihe Çalışkan & Sinan Saydam (2011): Experimental and Ab Initio Computational Studies on 4-(Benzhydryloxy)phthalonitrile, Molecular Crystals and Liquid Crystals, 537:1, 111-127

To link to this article: http://dx.doi.org/10.1080/15421406.2011.556412

Mol. Cryst. Liq. Cryst., Vol. 537: pp. 111–127, 2011

ISSN: 1542-1406 print/1563-5287 online
DOI: 10.1080/15421406.2011.556412

Taylor & Francis
Taylor & Francis Group

Experimental and *Ab Initio* Computational Studies on 4-(Benzhydryloxy)phthalonitrile

HANIFE SARAÇOĞLU,[1] FEYIZAN GÜNTEPE,[2] ÇIĞDEM YÜKSEKTEPE,[3] NEZIHE ÇALIŞKAN,[2] AND SINAN SAYDAM[4]

[1]Department of Middle Education, Educational Faculty, Ondokuz Mayis University, Kurupelit, Samsun, Turkey
[2]Department of Physics, Faculty of Arts and Sciences, Ondokuz Mayis University, Kurupelit, Samsun, Turkey
[3]Department of Physics, Faculty of Science, Çankırı Karatekin University, Ballıca, Çankırı, Turkey
[4]Department of Chemistry, Faculty of Science, Fırat University, Elazığ, Turkey

Molecular structure, atomic charges, dipole moments, total energies, and vibrational frequencies of 4-(benzhydryloxy)phthalonitrile in the ground state have been calculated using density functional theory (DFT) calculations and compared with the experimental data. Calculated frequencies are in good agreement with the corresponding experimental data. To determine conformational flexibility, the molecular energy profile of the title compound was obtained by semi-empirical (RAM1) calculations with respect to the selected torsion angle, which was varied from −180° to +180° in steps of 10°. In addition, frontier molecular orbitals (FMOs) analysis and thermodynamic properties of the title compound were investigated using theoretical calculations.

Keywords *ab initio* calculation; conformational analysis; frontier molecular orbitals; IR spectra; x-ray structure determination

Introduction

Substituted phthalonitriles have been used as starting materials for phthalocyanines [1]. Phthalocyanines (Pcs) have received much attention because of their synthetic and structural aspects, spectral properties, and electrochromic behavior [2–5]. Phthalocyanines, in particular their readily soluble peripherally substituted derivatives, possess a wide range of chemical and physical properties that make them interesting building blocks for a number of applications and new materials [2]. The properties of phthalocyanines such as high absorptivity in the near-infrared (IR) region, the ability to exhibit varying conductivities upon doping,

Address correspondence to Hanife Saraçoğlu, Department of Middle Education, Educational Faculty, Ondokuz Mayis University, 55139 Kurupelit, Samsun, Turkey. E-mail: hanifesa@omu.edu.tr

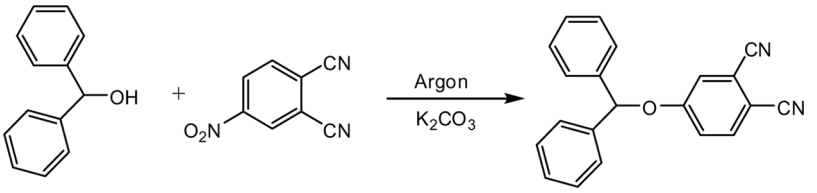

Scheme 1. Synthetic pathway for synthesis of the title compound.

and photocatalytic effects are due to the presence of highly conjugated π-electron systems [6]. The high absorptivity of phthalocyaninates at long wavelengths of the visible spectrum has received considerable attention as a probe for photodynamic therapy of tumors by laser [7].

4-(Benzhydryloxy)phthalonitrile is also a precursor in the synthesis of new phthalocyanines with various functional groups or macrocycles. We report the molecular and crystal structure of 4-(benzhydryloxy)phthalonitrile, determined by ^{1}H-nuclear magnetic resonance (NMR), IR, and X-ray studies, together with related theoretical calculations. The title compound has a different space group, $P2_1/c$, than a reported space group, $P2_1/n$ [8]. We performed X-ray crystallographic analysis of the title compound. We have also calculated geometric parameters of the molecule in the ground state to compare the results with the experimental geometric parameters using three different methods: RB3LYP/6-31G(d, p), RPBE1PBE/6-31G(d, p), and RB3PW91/6-31G(d, p). The conformational analysis of the title molecule with respect to selected torsion angle T(C1–C13–O1–C14) was performed using a RAM1 semi-empirical method. Finally, we calculated frontier molecular orbitals (FMOs) for the compound at RB3LYP/6-31G(d, p), RPBE1PBE/6-31G(d, p), and RB3PW91/6-31G(d, p).

Experiment

Synthesis of Compound 4-(Benzhydryloxy)phthalonitrile

The compound was synthesized according to reported procedures [9]. A mixture of 4-nitrophthalonitrile (0.173 g, 0.01 mol) and diphenylmethanol (1.84 g, 0.01 mol) was dissolved in 35 mL dry dimethylformamide (DMF) under argon atmosphere and the reaction was carried out at room temperature for 10 min. Then the temperature increased to 70°C–100°C, and (3.45 g, 0.025 mol) finely powdered dry K_2CO_3 added to the reaction mixture portionwise for 2 h. The reaction was carried out for 12 h under argon an atmosphere. Then the dark brown solution was poured into water and the pericipitate was filtered, washed with water, dried, and crystallized from ethanol. Yields 2.60 g (84%). ^{1}H NMR (dimethylsulfoxide, DMSO), δ(ppm): 6.3 singlet 1H, (CH), 7.2–7.7 multiplet 13H (aromatic CH). M.P. 152°C–154°C.

Measurement

IR spectra were recorded on an ATI Unicam-Mattson 1000 Fourier transform infrared (FTIR) spectrophotometer using KBr pellets. ^{1}H NMR spectra were obtained by using a Bruker 300 MHz spectrometer.

X-ray Crystallography

The data collection was performed at 293 K on a Stoe-IPDS-2 diffractometer equipped with a graphite monochromated Mo-K_α radiation ($\lambda = 0.71073$ Å). The structure was solved by a direct method using SHELXS-97 and refined by a full-matrix least-squares procedure using the SHELXL-97 program [10]. Molecular graphics were drawn by ORTEP-3 for Windows [11]. All nonhydrogen atoms were easily found from the difference Fourier map and refined anisotropically. All hydrogen atoms with carbons were included using a riding model and refined isotropically with C–H = 0.93 Å (for phenyl groups) and C–H = 0.98 Å, $U_{iso}(H) = 1.2U_{eq}(C)$.

DFT Calculations

Geometric optimization for the compound in the ground state (*in vacuo*) was performed on a personal computer using experimental geometry as input, employing the Gaussian 03 [12] program and Gaussview molecular visualization program at density functional theory (DFT) wave functions RB3LYP/6-31G(d, p), RPBE1PBE/6-31G(d, p), RB3PW91/6-31G(d, p) methods [13,14]. Then, we calculated vibrational frequencies for optimized molecular structures. To identify low energy conformation, selected degrees of torsion angle, T(C1–C13–O1–C14), were varied from −180° to +180° in steps of 10°, and the molecular energy profile was obtained at the semi-empirical RAM1 level.

Mulliken atomic charges were calculated at RB3LYP/6-31G(d, p), RPBE1PBE/6-31G(d, p) and RB3PW91/6-31G(d, p), levels. On the basis of vibrational analysis, the thermodynamic properties of the molecule at different temperatures were calculated. In addition, FMOs were carried out with the same level of theory for RB3LYP/6-31G(d, p), RPBE1PBE/6-31G(d, p), and RB3PW91/6-31G(d, p).

Results and Discussion

Description of the Crystal Structure

The compound crystallizes in the monoclinic space group $P2_1/c$. Details of crystal parameters, data collection, structure solution, and refinement are given in Table 1. The structure of the title compound is shown in Figure 1 [11]. The title compound contains three benzene rings. The dihedral angles between ring A(C1–C6), ring B(C7–C12), and ring C(C14–C19) with two cyano groups are 77.76(5)° (A/B), 8.88(6)° (A/C), and 76.11(5)° (B/C), respectively. The cyano bond distances, 1.137(2) Å and 1.138(2) Å, for C20≡N1 and C21≡N2 agree well with literature values [8,15]. The C–C≡N angles are almost linear and also show good agreement with literatue values [8,16].

Analysis of the crystal packing of the title compound and reported structure [8] shows significant differences. The reported structure is stabilized by π-π stacking interactions [8]. The title compound has both C–H . . . π and π-π interactions. Within the title compound, there is also an intramolecular C–H . . . O hydrogen bond (Table 2), with the O atom acting as an acceptor in the formation of an S(5) motif [17]. In crystal packing, no classical hyrogen bond is found. The title molecules are linked in a head to head fashion by π-π interactions. The aromatic ring A at (x, y, z) acts as a π-π interaction to ring C at (1 − x, −y, 1 − z), which centered at (1/2, 0, 1/2). Similarly, the aromatic ring at (x, 1/2 − y, − (1/2) + z) acts as a π-π interaction

Table 1. Crystallographic data for the title compound

Empirical formula	$C_{21}H_{14}N_2O$
Molecular weight	310.34
Temperature, T (K)	293
Wavelength (Å)	0.71073
Crystal system	monoclinic
Space group	$P2_1/c$
a (Å)	8.9048(5)
b (Å)	15.1095(10)
c (Å)	14.7759(9)
β (°)	124.695(4)
Volume, V (Å^3)	1634.56(17)
Z	4
Calculated density (g/cm^3)	1.261
F(000)	648
Crystal size (mm)	$0.600 \times 0.483 \times 0.400$
Θ range (°)	2.2/25.0
Index range (h, k, l)	−10/10, −17/17, −17/17
Reflections collected	7908
Independent reflections (R_{int})	2855(0.019)
Observed reflections [$I > 2\sigma(I)$]	2021
T_{min}, T_{max}	0.9616, 0.9814
Data/parameters	2855/218
Goodness-of-fit on F^2	1.03
Final R indices [$I > 2\sigma(I)$]	0.035
wR indices [$I > 2\sigma(I)$]	0.089
Largest diff. peak and hole (e. Å^{-3})	0.13 and −0.11

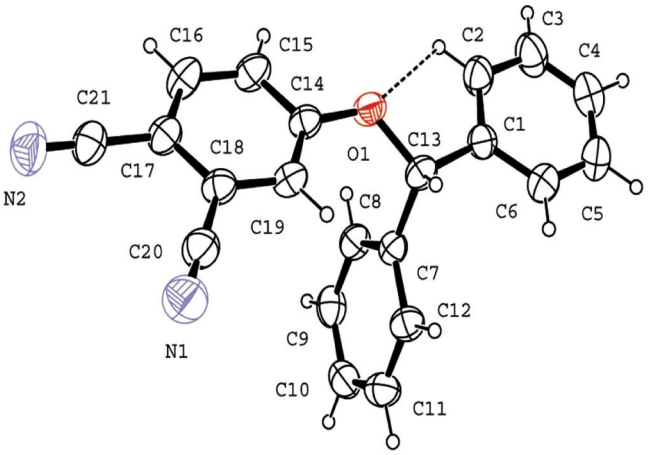

Figure 1. ORTEP drawing of the basic crystallographic unit, showing the atom-numbering scheme. Displacement ellipsoids are drawn at the 30% probability level and H atoms are shown as small spheres of arbitrary radii.

Table 2. Hydrogen bond geometries in crystal structure (Å, °)

D–H . . . A	D–H	H . . . A	D . . . A	D–H . . . A
C2–H2 . . . O1	0.93	2.35	2.703 (2)	102
C16-H16 . . . Cg2^{i}	0.93	2.72	3.6096 (19)	159

Cg2 is the centroid of the B ring.
Symmetry operation: (i) $1-x, 1/2+y, 1/2-z$.

to the ring at $(1-x, 1/2+y, 1/2-z)$, which centered at $(1/2, 1/2, 0)$. In this way, the special position of π-π interaction is centered at $(m+1/2, n, k+1/2)$ and $(m+1/2, n+1/2, k)$ (where m, n, and k independently take the value zero and integer). The C16 atom of phthalonitrile in the molecule at (x, y, z) acts as a hydrogen-bond donor, via atom H16, to the phenyl ring (B) of the cation at $(1-x, 1/2+y, 1/2-z)$, linking the chain along the b axis, as shown in Figure 2. In addition, the dimers are linked by a C–H . . . π intermolecular hydrogen bond.

Optimized Structure

The molecular structure of the title compound ($C_{21}H_{14}N_2O$) in the ground state (*in vacuo*) was optimized using DFT. Some selected geometric parameters experimentally obtained and theoretically calculated using three different methods (B3LYP,

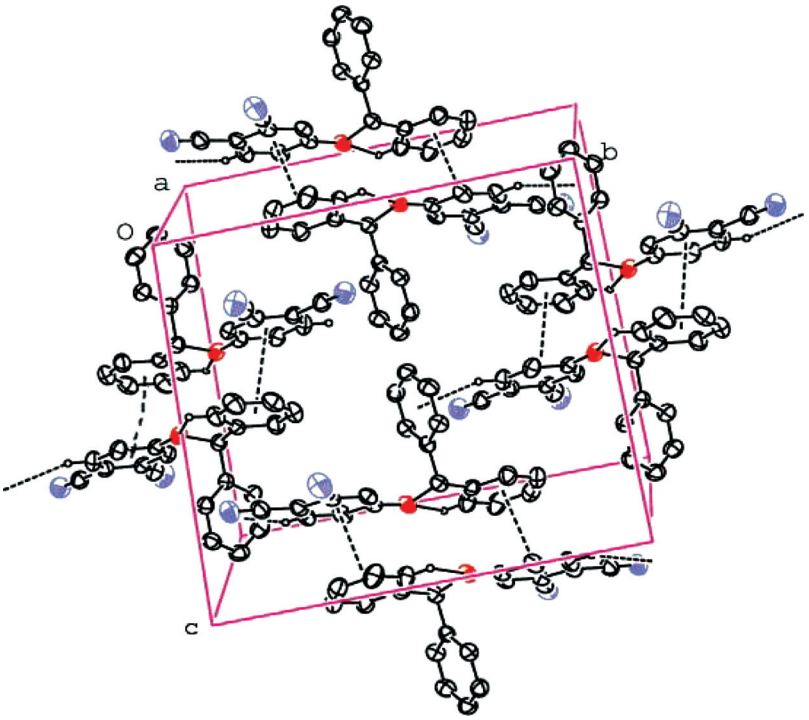

Figure 2. Packing of the title compound, showing hydrogen bonds and π-π stacking interactions. C-H hydrogens are omitted for clarity. Displacement ellipsoids are drawn at the 30% probability level.

Table 3. Selected geometrical parameters for X-ray structure and DFT methods

		DFT/6-31G(d, p)		
	Experimental	B3LYP	PBE1PBE	B3PW91
Bond lengths (Å)				
N1–C20	1.137 (2)	1.1628	1.1610	1.1628
N2–C21	1.138 (2)	1.1634	1.1616	1.1634
C18–C20	1.438 (2)	1.4341	1.4308	1.4315
C17–C21	1.435 (2)	1.4301	1.4268	1.4275
O1–C14	1.3615 (16)	1.3544	1.3468	1.3489
O1–C13	1.4460 (16)	1.4425	1.4357	1.4333
RMSE[a]		0.013	0.014	0.015
Max. difference[a]		0.026	0.024	0.026
Bond angles (°)				
N1–C20–C18	179.2 (2)	178.34	178.45	178.30
N2–C21–C17	178.54 (19)	178.36	178.44	178.33
C14–O1–C13	119.27 (11)	120.63	119.80	120.42
C1–C13–C7	111.18 (11)	112.39	114.60	112.06
O1–C13–C7	110.71 (10)	111.65	111.50	111.62
RMSE[a]		0.57	0.49	0.57
Max. difference[a]		1.36	3.42	1.15

[a]RMSE and maximum differences between the bond lengths and the bond angles computed by the theoretical method and those obtained from X-ray diffraction.

PBE1PBE, and B3PW91 with a 6-31G(d, p) basis set) are compared in Table 3. Using the root mean square error (RMSE) for evaluation, RB3LYP/6-31G(d, p) is the *ab initio* calculation that best predicts the bond distances, with a value of 0.013 Å. RPBE1PBE/6-31G(d, p) calculation provided the lowest RMSE for bond angles (0.49°). The highest RMSE for bond angles is obtained with a value of 0.57° for RB3LYP and RB3PW91.

The dihedral angles between optimized counterparts of the title compound are calculated at 73.24° (A/B), 29.07° (A/C), and 84.09° (B/C) for RB3LYP/6-31G(d, p); at 89.39° (A/B), 48.61° (A/C), and 87.62° (B/C) for RPBE1PBE/6-31G(d, p); and at 77.32° (A/B), 20.20° (A/C), and 83.00° (B/C) for RB3PW91/6-31G(d, p).

Vibrational Spectra

FTIR spectra were obtained in KBr discs using a Mattson 1000 FTIR spectrometer and are shown in Figure 3. Harmonic vibrational frequencies of the title compound were calculated using RB3LYP/6-31G(d, p), RPBE1PBE/6-31G(d, p), and RB3PW91/6-31G(d, p) methods and the obtained frequencies were not scaled. Vibrational bands assignments were made using the Gaussview molecular visualization program [12,13]. In order to facilitate assignment of the observed peaks we analyzed vibrational frequencies and compared our calculation of the title compound with experimental vibrational frequencies and these are shown in Table 4. It is known that *ab initio* calculations systematically overestimate the vibrational wavenumbers and discrepancies. We noted that the experimental results belong to the solid phase and theoretical calculations belong to the gaseous phase.

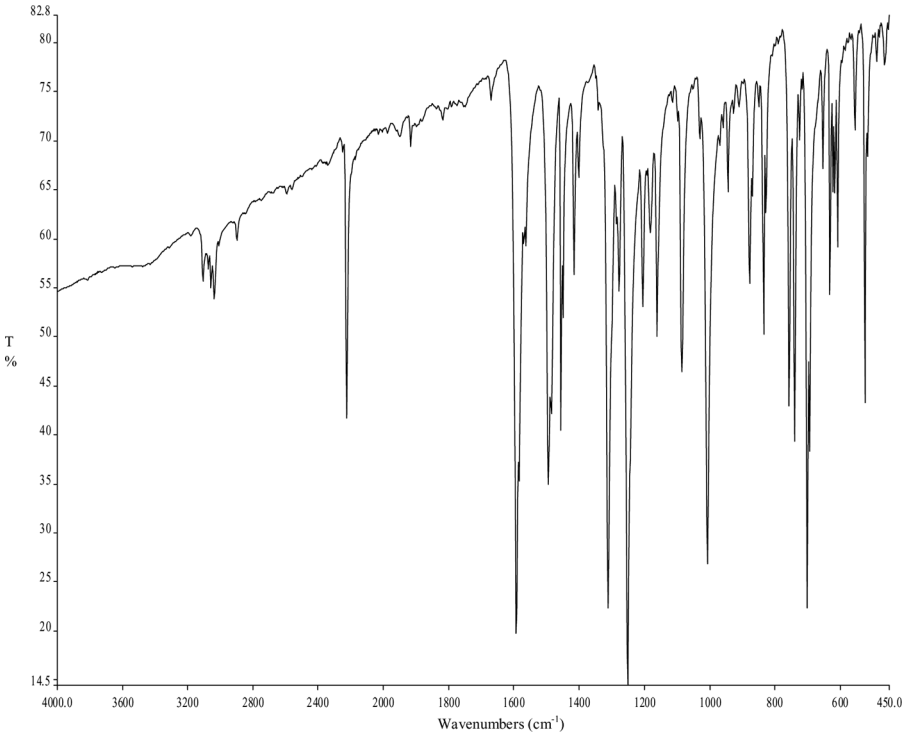

Figure 3. Experimental FTIR spectrum of the title compound.

The aromatic C-H stretching vibrations occur in the range of 3100–3000 cm^{-1} [18]. In the present study, the experimental C−H symmetric, asymmetric stretchings modes were observed at 3109, 3060, and 3039 cm^{-1}, respectively. As can be easily seen, the experimental values of C−H stretching modes are smaller than calculated frequencies, because the title compound is involved in hydrogen bonding. The experimental C≡N stretching mode was observed at 2226 cm^{-1}, and was calculated with RB3LYP/6-31G(d, p), RPBE1PBE/6-31G(d, p), and RB3PW91/6-31G(d, p) methods at 2348, 2381, and 2358 cm^{-1}, respectively. The characteristic C–O stretching vibration of the title structure was observed at 1008 cm^{-1}. The other calculated vibrational frequencies can be seen in Table 4. In general, when the calculated IR frequencies are compared with the experimental data of the title compound, all data agree with calculated vibrations.

Conformational Analysis

When the X-ray structure of the title compound is compared with its DFT-optimized counterparts (see Figure 4), conformational differences are shown between them. These differences are given an RMSE of 0.491 Å for RB3LYP/6-31G(d, p), 0.777 Å for RPBE1PBE/6-31G(d, p), and 0.429 Å for RB3PW91/6-31G(d, p). The calculated energy profile from RAM1 versus the torsion angle C1–C13–O1–C14 is given in Figure 5. The respective value of the selected degree of torsion angle, T(C1–C13–O1–C14), is 177.8° in the X-ray structure, whereas the corresponding

Table 4. Comparison of the observed and calculated vibrational spectra of the title compound

		DFT/6-31G(d, p)		
Assignment	Experimental	B3LYP	PBE1PBE	B3PW91
ν_s C-H (aromatic)	—	3223	—	3237
ν_s C-H (aromatic)	3109	3213	3239	3224
ν_{as} C-H (aromatic)	—	3208	3234	3220
ν_{as} C-H (aromatic)	—	3205	3232	3216
ν_{as} C-H (aromatic)	—	3196	3227	3208
ν_{as} C-H (aromatic)	—	3176	3223	3207
ν_{as} C-H (aromatic)	3060	3168	3218	3189
ν_{as} C-H (aromatic)	3039	—	3196	3176
ν C-H (aliphatic)	—	3035	3029	3034
ν C≡N	—	2354	2386	2363
ν C≡N	2226	2348	2381	2358
ν C-C (aromatic)	—	1658	1687	1670
ν C-C (aromatic)	1593	1651	1678	1664
ν C-C (aromatic)	—	1643	1669	1654
ν C-C (aromatic)	—	1642	1668	1616
ν C-C (aromatic)	—	1603	1633	—
γ CH (aromatic)	1496	1541	1554	1544
γ CH (aromatic)	1457	1538	1548	1540
γ CH (aromatic)	—	1537	1546	1537
γ CH (aromatic) + γ CH (aliphatic)	1451	1497	1504	1497
γ CH (aromatic)	1417	—	1498	1492
ν C-C(aromatic)	1402	1451	1470	1458
γ CH (aliphatic) + ν C-C (aromatic)	—	—	1404	1394
γ CH (aliphatic)	—	1389	—	—
ν C-C (aromatic)	—	—	1395	1384
ν C-C (aromatic)	—	—	1389	—
ν C-C (aromatic) + γ CH (aliphatic)	—	—	—	1382
γ CH (aromatic) + γ CH (aliphatic)	—	—	1375	1371
γ CH (aromatic)	—	1366	—	—
γ CH (aliphatic) + ν C-C (aromatic) + γ CH (aromatic)	—	1363	—	—
γ CH (aromatic)	—	1362	—	—
γ CH (aromatic) + γ CH (aliphatic)	—	—	—	1361
γ CH (aliphatic)	—	—	1359	—

(*Continued*)

Table 4. Continued

Assignment	Experimental	DFT/6-31G(d, p)		
		B3LYP	PBE1PBE	B3PW91
γ CH (aromatic)	—	—	1348	—
γ CH (aromatic) + γ CH (aliphatic)	—	1335	—	1338
γ CH (aromatic) + γ CH (aliphatic)	1278	1315	1327	1322
γ CH (aromatic) + γ CH (aliphatic)	—	1297	1315	1300
γ CH (aromatic)	1252	1283	1290	1285
γ CH (aromatic)	1206	1238	1251	1242
γ CH (aromatic) + γ CH (aliphatic)	1183	—	1237	—
α CH (aromatic)	—	—	1222	1216
α CH (aromatic)	—	1207	1211	1206
α CH (aromatic)	—	1204	1206	1205
α CH (aromatic)	1163	1195	1200	1197
α CH (aromatic)	—	1120	1123	1123
α CH (aromatic)	1086	1115	1120	1116
α CH (aromatic)	—	1058	1070	1065
α CH (aromatic)	1031	1056	1068	1061
ν C-O	1008	1035	1055	1053
θ (aromatic)	—	1017	1021	1016
θ (aromatic)	—	—	1020	1015
δ CH (aromatic)	—	706	26.69	—
δ CH (aromatic)	—	—	989	—
δ CH (aromatic)	946	—	987	978
δ CH (aromatic)	—	971	—	—
δ CH (aromatic)	—	—	939	—
δ CH (aromatic)	—	655	41.16	652
δ CH (aromatic) + β CH (aromatic)	912	887	902	889
β CH (aromatic)	879	874	878	849
ω CH (aromatic)	836	852	858	849
ω CH (aromatic)	829	846	856	846
ω CH (aromatic)	758	776	783	774
ω CH (aromatic)	741	761	762	758
ω CH (aromatic) + θ (aromatic)	—	751	752	753
θ (aromatic)	726	741	741	742
ω CH (aromatic)	703	720	720	718
ω CH (aromatic)	695	709	714	709
β C-C≡N + θ (aromatic)	655	663	665	661

(*Continued*)

Table 4. Continued

Assignment	Experimental	DFT/6-31G(d, p)		
		B3LYP	PBE1PBE	B3PW91
β C-C≡N + θ (aromatic)	633	642	647	641
δ CH (aromatic)	623	640	646	640
θ (aromatic)	618	633	633	630
β C-C≡N + θ (aromatic)	610	624	627	623
ω CH (aromatic) + β C-C≡N	557	571	—	568
ω CH (aromatic)	526	548	552	549
β C-C≡N + β C-O-C	490	522	528	524
ω CH (aromatic)	467	—	—	—

Vibrational modes: ν, stretching; β, bending; α, scissoring; γ, rocking; ω, wagging; δ, twisting; θ, ring breathing; s, symmetric; as, asymmetric.

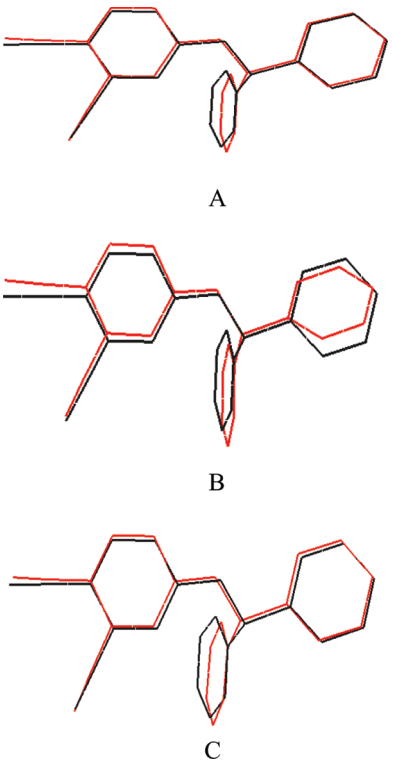

Figure 4. Atom-by-atom superimposition of the structures calculated (red) (A = B3LYP/6-31G(d, p), B = PBE1PBE/6-31G(d, p), and C = B3PW91/6-31G(d, p) over the X-ray structure (black) for the title compound. Hydrogen atoms omitted for clarity.

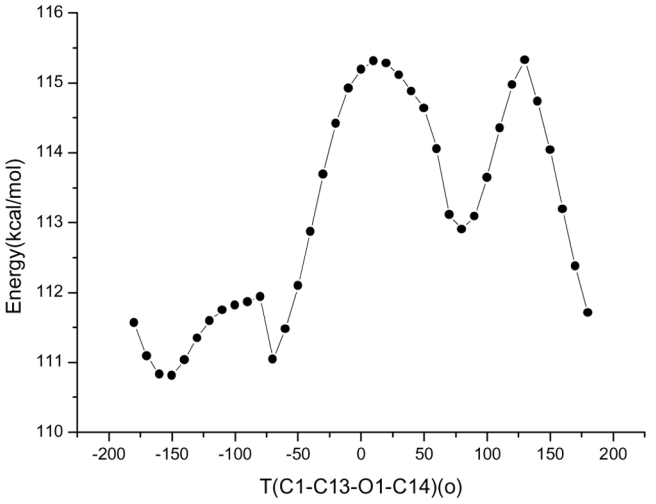

Figure 5. Molecular energy profile of the optimized counterpart of the title compound versus selected degrees of torsion angle.

value in optimized geometry is −161.2° for RB3LYP/6-31G(d, p), −160.3° for RPBE1PBE/6-31G(d, p), and −161.8° for RB3PW91/6-31G(d, p). According to Figure 5, the minimum energy is located at −150° (energy of 110.812 kcal mol^{-1}), the maximum energy is located at 130° (energy of 115.326 kcal mol^{-1}). The energy difference between the most favorable and unfavorable conformers, which arises from rotational potential barrier calculated with respect to the selected torsion angle, was calculated as 4.514 kcal mol^{-1} when both selected degrees of torsion angle are considered. The conformations with maximum and minimum energy are shown in Figures 6a and 6b, respectively. When Figures 6a and 6b are compared, ring B and ring C in Figure 6b are closer than in Figure 6a. In Figure 6b, the atom–atom distances of ring B and ring C are smaller than those in Figure 6a. Whereas the distances of C7 . . . C14 and C6 . . . O1 atoms are 2.754 and 2.772 Å in Figure 6b, the same distances in Figure 6a are 3.177 and 3.594 Å. Therefore, the electrostatic repulsions are increased in the title molecule, and the energy of the system is also increased. Conversely, the distance of the C2 . . . O1 atom (3.624 Å) in Figure 6b is

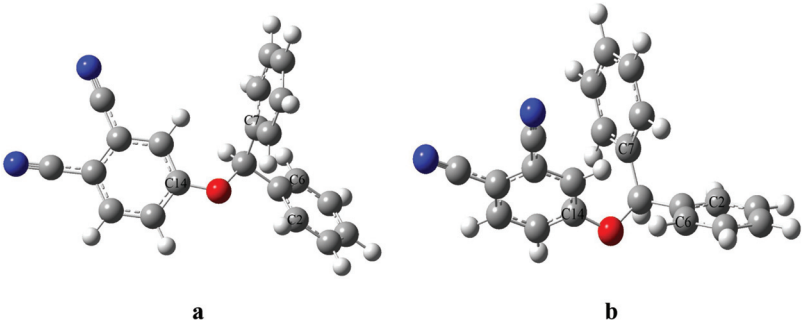

Figure 6. (a) Molecular structure at −150°; (b) Molecular structure at 130°.

greater than in Figure 6a (2.752 Å). The difference between experimental (Figure 1) and calculated conformers (Figure 6a) can occur intra-molecular hydrogen bond.

The molecular energy can be divided into bonded and nonbonded contributions. The bonded energy is considered to be independent of torsional angle changes and therefore vanishes when relative conformer energies are calculated. The nonbonded energy is further separated into torsional steric and electrostatic terms [19]. The title compound contains an intramolecular hydrogen bond, and it can be deduced from the computational results that the most stable conformer of the title compound is principally determined by the nonbonded torsional energy and electrostatic energy terms affected by packing of the molecules. Because the reported structure has no intramolecular hydrogen bond, it is less resistant to rotation about this torsion angle, so it can be expected to show better agreement with the calculated torsion angle.

Mulliken Atomic Charges and Frontier Molecular Orbitals

The Mulliken atomic charges were calculated with RB3LYP/6-31G(d, p), PBE1PBE/6-31G(d, p), and B3PW91/6-31G(d, p) methods and illustrated in Table 5. Atomic charge analysis revealed that the negative charges on the oxygen atom and nitrogen atoms are significantly greater than on the other atoms. In the C2–H2 . . . O1 intramolecular hydrogen bond, the mean charge distributions of C2, H2, and O1 are −0.12, 0.12, and −0.54, respectively. These values from DFT method are fairly suitable to explain electrostatic interactions between intra-acting atoms.

The FMOs are important in determining such properties as molecular reactivity and the ability of a molecule to absorb light. These FMOs are very important for optical and electric properties [20]. The molecular orbital (MO) calculations indicate that the title compound has 81 occupied MOs. The distributions and energy levels of the HOMO-1, HOMO, LUMO, and LUMO +1 orbitals computed at the RB3LYP/6-31G(d, p), RPBE1PBE/6-31G(d, p), and RB3PW91/6-31G(d, p) levels for the title compound are shown in Figures 7a, 7b, and 7c. The HOMOs and HOMO-1s for RB3LYP/6-31G(d, p) and RB3PW91/6-31G(d, p) levels have approximately similar shapes and seem to be the π-bonding-type orbitals. The electron clouds of the HOMO-1s are localized on rings A(C1-C6) and C(C14-C19), and those of the HOMOs are localized on rings A(C1-C6) and B(C7-C12). But HOMOs and HOMO-1s are different shapes for the RPBE1PBE/6-31G(d, p) level. The LUMOs and LUMO + 1s for three methods have the same locations, whereas the HOMOs and HOMO-1s are different. LUMOs and LUMO + 1s orbitals are mainly localized on ring C with two cyano groups. In all cases, LUMOs are π^*-anti-bonding orbitals. HOMO and LUMO energies, the energy gap, total energies, and dipole moments of the title compound for the three methods were calculated and are given in Table 6.

An electronic system with a larger HOMO-LUMO gap should be less reactive than one having a smaller gap [21]. The HOMO-LUMO gap values of the molecule are between 4.79 and 5.20 eV as seen in Table 6. In addition, the intermolecular interactions have a significant influence in decreasing the HOMO-LUMO gaps in solids [22,23].

Thermodynamic Properties

On the basis of vibrational analysis at the RB3LYP/6-31G(d, p) level, the standard statistical thermodynamic functions, viz. standard heat capacity ($C^0_{p,m}$), standard

Table 5. Mulliken atomic charges of the title compound

Atom	B3LYP/6-31G(d, p)	PBE1PBE/6-31G(d, p)	B3PW91/6-31G(d, p)
O1	−0.547	−0.539	−0.546
N1	−0.467	−0.466	−0.482
N2	−0.471	−0.470	−0.486
C1	0.093	0.040	0.054
C2	−0.104	−0.116	−0.130
H2	0.097	0.133	0.134
C3	−0.090	−0.135	−0.128
H3	0.091	0.133	0.126
C4	−0.080	−0.118	−0.115
H4	0.091	0.132	0.126
C5	−0.088	−0.138	−0.126
H5	0.092	0.133	0.128
C6	−0.107	−0.131	−0.126
H6	0.082	0.142	0.120
C7	0.120	−0.002	0.094
C8	−0.107	−0.115	−0.127
H8	0.096	0.145	0.135
C9	−0.083	−0.129	−0.120
H9	0.095	0.138	0.131
C10	−0.081	−0.121	−0.116
H10	0.095	0.138	0.132
C11	−0.085	−0.127	−0.123
H11	0.097	0.140	0.134
C12	−0.125	−0.144	−0.156
H12	0.086	0.135	0.123
C13	0.040	0.036	0.019
H13	0.107	0.151	0.142
C14	0.372	0.366	0.372
C15	−0.113	−0.156	−0.150
H15	0.119	0.164	0.157
C16	−0.091	−0.113	−0.115
H16	0.128	0.170	0.166
C17	0.140	0.091	0.112
C18	0.126	0.077	0.097
C19	−0.117	−0.128	−0.131
H19	0.130	0.171	0.163
C20	0.233	0.259	0.263
C21	0.224	0.250	0.254

entropy (S_m^0), and standard enthalpy ($H_{p,m}^0$) for the title compound, were obtained from the theoretical frequencies and are listed in Table 7.

From Table 7, we can find that the standard heat capacities, entropies and enthalpies are increasing with temperatures ranging from 100 to 1000 K due to the fact that the vibrational intensities of molecules increase with temperature. The correlation equations between these thermodynamic properties and temperature T are

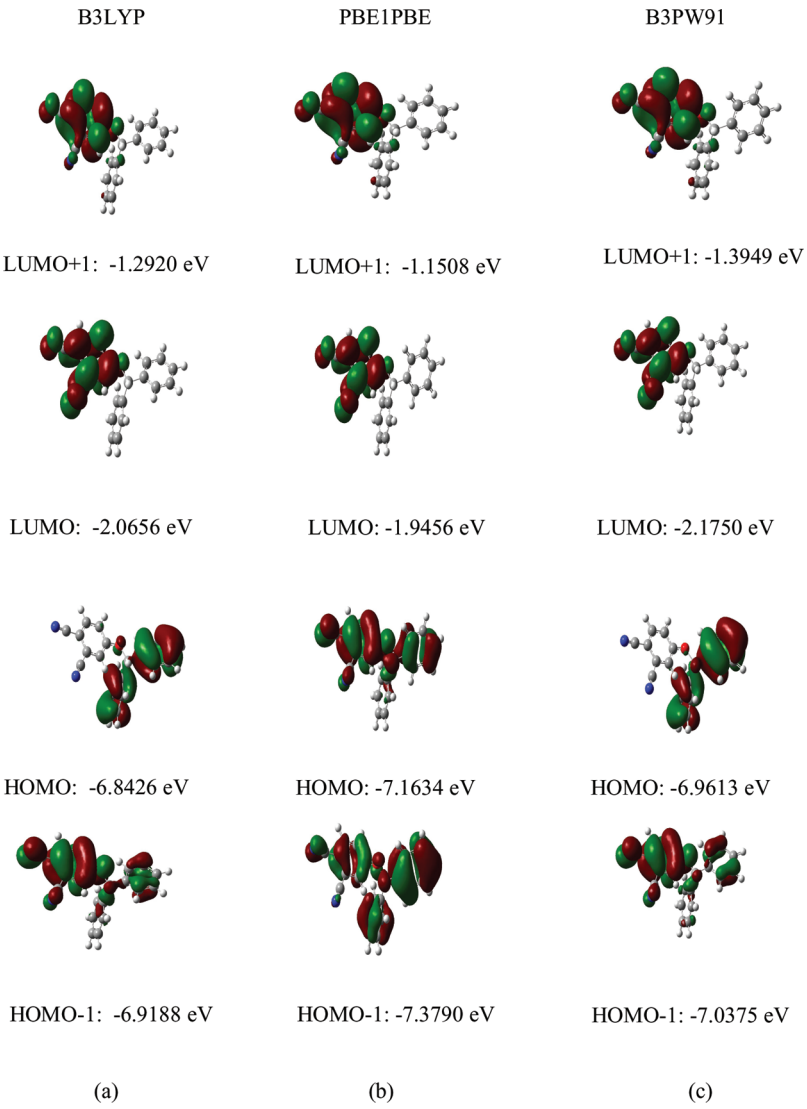

Figure 7. Plots of the frontier orbitals of the title compound for three different methods.

Table 6. Calculated energy values and dipole moments in the title compound

Orbital	B3LYP/ 6-31G(d, p)	PBE1PBE/ 6-31G(d, p)	B3PW91/ 6-31G(d, p)
HOMO (a.u.)	−0.252	−0.263	−0.256
LUMO (a.u.)	−0.076	−0.072	−0.080
Δ (a.u.) (eV)	0.176(4.79)	0.191(5.20)	0.176(4.79)
Total energies (a.u.)	−993.4	−992.2	−993.0
Dipol moments (D)	8.309	8.312	8.274

Table 7. Thermodynamic properties of the title compound at different temperatures at B3LYP/6-31G(d, p) method

T (K)	$C^0_{p,m}$ ($cal \cdot mol^{-1} \cdot K^{-1}$)	S^0_m ($cal \cdot mol^{-1} \cdot K^{-1}$)	H^0_m ($kcal \cdot mol^{-1}$)
100.00	30.637	97.130	2.179
200.00	52.074	126.073	6.477
298.15	75.882	152.074	12.946
300.00	76.329	152.556	13.091
400.00	99.114	178.282	22.088
500.00	118.159	202.963	33.184
600.00	133.436	226.271	45.991
700.00	145.685	248.100	60.168
800.00	155.642	268.491	75.449
900.00	163.858	287.546	91.636
1000.00	170.724	305.386	108.574

as follows:

$$C^0_{p,m} = 0.11414 + 0.29578T - 1.2559 \times 10^{-4}T^2 \qquad (R^2 = 0.99921) \quad (1)$$

$$S^0_m = 67.45188 + 0.30416T - 6.61596 \times 10^{-5}T^2 \qquad (R^2 = 0.99999) \quad (2)$$

$$H^0_m = -3.29875 + 0.03371T + 7.9372 \times 10^{-5}T^2 \qquad (R^2 = 0.99943) \quad (3)$$

All of the thermodynamic data provide helpful information for further study of the title compound. They can be used to compute the other thermodynamic energies according to relationships of thermodynamic functions and estimate the directions of chemical reactions according to the second law of thermodynamics in the thermochemical field [24].

Conclusions

In this work, the title compound was characterized by ^{1}H NMR, X-ray analysis, and FTIR spectra. The X-ray structure was found to be very slightly different from its optimized counterparts, and the crystal structure is stabilized by C–H$\ldots\pi$ and π-π interactions. It was noted that the experimental results belong to the solid phase and theoretical calculations belong to the gaseous phase. In the solid state, the existence of the crystal field along with the intra- and intermolecular interactions have connected the molecules together, which is presumably responsible for the discrepancies of bond parameters between the calculated and experimental values. Despite the differences observed in the geometric parameters, the general agreement is good and the theoretical calculations support the solid-state structures. The theoretical vibrational spectrum assignments of 4-(benzhydryloxy)phthalonitrile, $C_{21}H_{14}N_2O$, were calculated and the experimental vibrational spectrum assignments of the title compound were compared with theoretical results. Computed spectra seemed to be in a good agreement with experimental results. The energy gap value of the title compound is between 4.79 and 5.20 eV. This result indicates that the title structure is

quite stable. The energy levels between HOMO and LUMO should be expected to occur with π-π^* transitions. The correlations between the thermodynamic properties $C^0_{p,m}, S^0_m, H^0_m$ and temperatures T were also obtained. These calculations and the thermodynamic data will provide helpful information for further studies of the title compound.

Supplementary Data

Crystallographic data for the structural analysis have been deposited with the Cambridge Crystallographic Data Centre, CCDC No. 723055. Copies of this information may be obtained free of charge from the Director, CCDC, 12 Union Road, Cambridge CB2 1EZ, UK (fax: +44-1223-336033; E-mail: deposit@ccdc.cam.ac.uk; or http://www.ccdc.cam.ac.uk).

Acknowledgment

The authors acknowledge the Faculty of Arts and Sciences, Ondokuz Mayis University, Turkey, for the use of the STOE IPDS-II diffractometer (purchased under grant F.279 of the University Research Fund).

References

[1] McKeown, N. B. (1998). *Phthalocyanine Materials: Synthesis, Structure and Function*, Cambridge University Press, Cambridge, 275.
[2] Leznoff, C. C., & Lever, A. B. P. (1989–1993). *Phthalocyanines: Properties & Applications, Vols. 1 and 2*. VHC Publishers: Weinheim and New York.
[3] Moser, F. H., & Thomas, A. L. (1983). *The Phthalocyanines, Vols. 1 and 2*. CRC Press: Boca Raton, FL.
[4] Stillmann, M. J., & Nyokong, T. (1989). In: *Phthalocyanines: Properties and Applications*, Leznoff, C. C. & Lever, A. B. P. (Eds.), VCH: Weinheim, Germany.
[5] Toshima, N., Kawamura, S., & Tominaga, T. (1993). *Chem. Lett.*, no. 8 1299.
[6] Schultz, H., Lehman, H., Rein, M., & Hanack, M. (1991). *Struct. and Bond.*, *74*, 41.
[7] Rosenthal, I., Ben-Hur, E., Greenberg, S., Concepcion-Lam, A., Drew, M. D., & Leznoff, C. C. (1991). *Photochem. Photobiol.*, *46*, 959.
[8] Petek, H., Akdemir, N., Ağar, E., Özil, M., & Şenel, I. (2004). *Acta Cryst.*, *E60*, o1105.
[9] Leznoff, C. C., Hu, M., McArthur, C. R., & Qin, Y. (1994). *Can. J. Chem.*, *72*, 1990.
[10] Sheldrick, G. M. (1997). *SHELXS-97 and SHELXL-97*, University of Gottingen: Gottingen, Germany.
[11] Farrugia, L. J. (1997). *J. Appl. Crystallogr.*, *30*, 565.
[12] Frisch, M. J., Trucks, G. W., Schlegel, H. B., Scuseria, G. E., Robb, M. A., Cheeseman, J. R., Montgomery, J. A., Vreven, T., Kudin, K. N., Burant, J. C., Millam, J. M., Iyengar, S. S., Tomasi, J., Barone, V., Mennucci, B., Cossi, M., Scalmani, G., Rega, N., Petersson, G. A., Nakatsuji, H., Hada, M., Ehara, M., Toyota, K., Fukuda, R., Hasegawa, J., Ishida, M., Nakajima, T., Honda, Y., Kitao, O., Nakai, H., Klene, M., Li, X., Knox, J. E., Hratchian, H. P., Cross, J. B., Adamo, C., Jaramillo, J., Gomperts, R., Stratmann, R. E., Yazyev, O., Austin, A. J., Cammi, R., Pomelli, C., Ochterski, J. W., Ayala, P. Y., Morokuma, K., Voth, G. A., Salvador, P., Dannenberg, J. J., Zakrzewski, V. G., Dapprich, S., Daniels, A. D., Strain, M. C., Farkas, O., Malick, D. K., Rabuck, A. D., Raghavachari, K., Foresman, J. B., Ortiz, J. V., Cui, Q., Baboul, A. G., Clifford, S., Cioslowski, J., Stefanov, B. B., Liu, G., Liashenko, A., Piskorz, P., Komaromi, I., Martin, R., Fox, D. J., Keith, T., Al-Laham, M. A., Peng, C. Y., Nanayakkara, A.,

Challacombe, M., Gill, P. M. W., Johnson, B., Chen, W., Wong, M. W., Gonzalez, C., & Pople, J. A. (2004). *Gaussian 03*, Gaussian, Inc.: Wallingford, CT.
[13] Dennington, R. I. I., Keith, T., & Millam, J. (2007). *GaussView, Ver. 4.1.2*, Semichem Inc.: Shawnee Mission, KS, USA.
[14] Frisch, A., Dennington, R. I. I., Keith, T., Millam, J., Neilsen, A. B., Holder, A. J., *et al.* (2007). *GaussView Reference, Ver. 4.0*, Gaussian, Inc.: Pittsburg, PA.
[15] Allen, F. H., Kennard, O., Watson, D. G., Brammer, L., Orpen, A. G., & Taylor, R. (1987). *J. Chem. Soc. Perkin Trans.*, *2*, 19.
[16] Chopra, D., Mohan, T. P., Vishalakshi, B., & Guru Row, T. N. (2006). *Acta Cryst.*, *C62*, o540.
[17] Bernstein, J., Davis, R. E., Shimoni, L., & Chang, N. L. (1995). *Angew. Chem. Int. Ed. Engl.*, *34*, 1555.
[18] Roeges, N. P. G. (1994). *A Guide to the Complete Interpretation of Infrared Spectra of Organic Structures*, Wiley; New York.
[19] Weiqun, Z., Baolong, L., Yang, C., Yong, Z., & Xujie, L. L. Y. (2005). *J. Mol. Struct. Theochem.*, *715*, 117.
[20] Fleming, I. (1976). *Frontier orbitals and organic chemical reactions*, Wiley: London.
[21] Kurtaran, R., Odabaşoğlu, S., Azizoğlu, A., Kara, H., & Atakol, O. (2007). *Polyhedron*, *26*, 5069.
[22] Zheng, S.-L., Zhang, J.-P., Chen, X.-M., Huang, Z.-L., Lin, Z.-Y., & Wong, W.-T. (2003). *Chem. Eur. J.*, *9*, 3888.
[23] Zheng, S.-L., Zhang, J.-P., Wong, W.-T., & Chen, X.-M. (2003). *J. Am. Chem. Soc.*, *125*, 6882.
[24] Sun, Y.-X., Wei, W.-X., Hao, Q.-L., Lu, L.-D., & Wang, X. (2009). *Spect. Acta Part.*, *A73*, 772.